Multi-Modes Multiscale Approach of Heat Transfer Problems in Heterogeneous Solids with Uncertain Thermal Conductivity

Shan Zhang[1], Zihao Yang[2] and Xiaofei Guan[3,*]

[1] *College of Mathematics and Physics, Shanghai University of Electric Power,*
Shanghai 200090, China
[2] *School of Mathematics and Statistics, Northwestern Polytechnical University, Xi'an,*
Shanxi 710072, China
[3] *School of Mathematical Sciences, Tongji University, Shanghai 200092, China*

Abstract. Stochastic temperature distribution should be carefully inspected in the thermal-failure design of heterogeneous solids with unexpected random energy excitations. Stochastic multiscale modeling for these problems involve multiscale and high-dimensional uncertain thermal parameters, which remains limitation of prohibitive computation. In this paper, we propose a multi-modes based constrained energy minimization generalized multiscale finite element method (MCEM-GMsFEM), which can transform the original stochastic multiscale model into a series of recursive multiscale models sharing the same deterministic material parameters by multiscale analysis. Thus, MCEM-GMsFEM reveals an inherent low-dimensional representation in random space, and is designed to effectively reduce the complexity of repeated computation of discretized multiscale systems. In addition, the convergence analysis is established, and the optimal error estimates are derived. Finally, several typical random fluctuations on multiscale thermal conductivity are considered to validate the theoretical results in the numerical examples. The numerical results indicate that the multi-modes multiscale approach is a robust integrated method with the excellent performance.

AMS subject classifications: 65N12, 65N15, 80M10, 80M22

Key words: Stochastic multiscale heat transfer problems, uncertainty quantification, MCEM-GMsFEM, multimodes expansion.

1 Introduction

Heterogeneous solids are widely used in engineering practice, and are often exposed to strong temperature changes, such as thermal protection systems for space aircraft [1]

---

*Corresponding author.
Email:* guanxf@tongji.edu.cn (X. Guan)

and thermal coating for microelectronic systems [2], etc. Under severe thermal conditions, accurate and efficient prediction of the damage or fracture process of heterogeneous solids requires a comprehensive understanding of the uncertainty propagation of temperature fields under a multiscale framework [3, 4], where stochasticity comes from morphological randomness or material uncertainty [5], such as mismatches between the micro components due to their dispersion and orientation, stochastic cracks or defects, measurement errors or incomplete cognition of thermal expansion and conduction parameters [6]. Therefore, developing a new reliable and effective uncertainty quantification method for multiscale heat transfer problem [7, 8] is of paramount importance and practical significance, and this method can both capture all stochastic responds with high efficient simulations and alleviate the computational cost.

Accounting for the uncertainty is a type of classic issue in the numerical computation of random medium [9]. Due to the high-dimensional nature of the random space, many theories have been developed to deal with the problems. Monte Carlo method and its variants [10] are usually used to solve the governing equation of stochastic problems, in which the uncertainty is sampled by use of the probability distribution function or the random field, and then the corresponding stochastic problem is approximated by a series of deterministic problems, statistical information of their exact solutions can be obtained subsequently. Another typical methods are to approximate the physical quantities of interest in the random space and physical space, respectively. These include the stochastic Galerkin method [11, 12] and stochastic collocation method [13, 14], etc. The uncertainty is generally represented in the random space through Wiener chaos expansion, generalized polynomial chaos expansion or collocation points. Here, the stochastic collocation method combining the advantages of stochastic finite element method and Monte Carlo sampling, has received wide attention, where the collocation points can be chosen with full tensor product method [15] and Smolyak sparse grid method [13] etc. In [16–20], the multi-modes Monte Carlo method is successfully applied to solve various important stochastic problems. Through these methods, the computation saving is obtained by the dimensinality reduction. It should be pointed out that the multiscale modeling and computational method of stochastic heat conduction problem in the high-dimensional uncertainty space is still extremely challenging due to their complex correlative nature.

Except for uncertainties of thermal conductivity, it is also necessary to consider its multiscale features in heterogeneous solids. This leads to tremendous cost for solving the stochastic multiscale heat transfer problem by use of traditional numerical methods. Therefore, numerous researchers have begun to pay attention to the design of the multiscale models and computation methods, which can efficiently reduce the complex fine-scale problems to coarse-scale problems, including homogenization method [21–24], variational multiscale method (VMM) [25–28], upscaling method [29–31], heterogeneous multiscale methods (HMM) [32], and multiscale finite element method (MsFEM) [33–39]. Moreover, when the uncertainties are integrated into the multiscale model, some attempts have been made to deal with the coupling of the multiscale and uncertainty characteristics of stochastic multiscale problem [26, 40–44]. [45] proposed a stochastic mul-

tiscale method to quantify the most significant input parameters influencing the thermal conductivity of polymeric nano-composites with clay reinforcement. [46] presented a new stochastic multiscale analysis approach to analyze the heat transfer performance of heterogeneous materials with random structures at different length scales. [47] proposed a hybrid machine learning method to predict the thermal conductivity of polymeric nanocomposites. In [4], a probabilistic surrogate model had been proposed to quantify the uncertainty in thermal conductivity computations due to molecular dynamics noise, and its effect on the computation of the temperature distribution in heat conduction simulations. [3] developed a novel multiscale computational method for heat conduction problems of composite structures with diverse periodic configurations in different subdomains. While most studies are based on deterministic approaches, there is a comparatively lower number of stochastic multiscale methods accounting for morphological and material uncertainties simultaneously. Thus, it is necessary to design better algorithms to solve the multiscale model of stochastic heat transfer problem, where uncertainties in morphology and materials need to be taken into account for reliable predictions.

When the physical and mechanical analysis of heterogeneous solids (e.g., concerete materials) are carried out in some applications, the CEM-GMsFEM [33,34] exhibits a very important advantage that it is free of the assumption regarding the distinct separation of the different length scales, where the relationship between aggregation diameters and interface thicknesses must be considered. Moreover, the natural parallelization without any special amendments, which only some independent problems solved with neighboring subdomains, guarantees a substantial speed-up to the computations. Inspired by the multi-modes methods, the primary objective of this paper is to develop and design a general stochastic multiscale framework and better algorithm to capture the influence of numerous uncertain geometrical and material parameters on the stochastic temperature and heat flux distribution of heterogeneous solids. The main idea is to reformulate the original stochastic multiscale heat transfer problem to a series of recursive multiscale model with same deterministic multiscale material parameters by use of the multi-modes method [16,17]. For each multiscale model with deterministic material parameters, CEM-GMsFEM is employed to reduced the computation cost. In particular, in view of the same features of the coefficient matrix shared by all multiscale models after multi-modes expansion, LU decomposition can be reused to effectively reduce the complexity of repeated computation of discretized multiscale systems, which leads a significant computation saving overall numerical method. In addition, incorporating the merits of CEM-GMsFEM and multi-mode method, the convergence of MCEM-GMsFEM is also established with linearly dependent on the mesh size and independent of contrast.

This paper is organized as follows. In Section 2, multi-modes multiscale analysis and the formulae of MCEM-GMsFEM are proposed, and the corresponding numerical algorithms are built. In Section 3, convergence analysis is established, and the optimal error estimates are derived in detail. In Section 4, some numerical examples are demonstrated to confirm the theoretical analysis, and some conclusions are given in Section 5.

2 Multi-modes multiscale analysis

2.1 Governing equations

Consider a heterogeneous solid in domain D subjected to extrinsic and intrinsic random excitations, and it is originally in equilibrium at a uniform temperature T_0 on ∂D, where $D \subset \mathbb{R}^d$ ($d \geq 1$) is a convex bounded polygonal domain with Lipschitz continuous boundary ∂D. The heat flux q through a heterogeneous solid by conduction can usually be described by Fourier's law, which is stated by

$$q(x,\xi) = -\kappa(x,\xi)\nabla T^\varepsilon(x,\xi) \quad \text{in } D \times \Omega, \tag{2.1}$$

where $\xi \in \Omega$, and $x \in D$ is the cartesian coordinates. $(\Omega, \mathcal{F}, \mathbb{P})$ is a complete probability space, and Ω is the sample space, $\mathcal{F}$ is the subspace of σ-algebra in Ω, $\mathbb{P}: \mathcal{F} \to [0,1]$ is the probability measure. The $\kappa(x,\xi)$ is referred to as the thermal conductivity of the heterogeneous solids with multiscale and uncertain characteristics. The temperature $T^\varepsilon: \overline{D} \times \Omega \to \mathbb{R}$ is the real-valued random function defined on Ω. Fourier's law presents a phenomenological linear relationship between q and $\nabla T^\varepsilon(x,\xi)$, which will be highly accurate providing that the characteristic length scale of the temperature gradient is significantly larger than the microscopic length scale of the heterogeneous solids (i.e., the molecular length scale). Practically most engineering applications will fall into this category, with the exception being heat transfer in highly nonequilibrium conditions (i.e., the heterogeneous solids under laser heating).

From the first law of thermodynamics, a general heat transfer problem is given as:

$$\rho c \frac{\partial T^\varepsilon(x,\xi)}{\partial t} + \nabla \cdot q(x,\xi) = f(x,\xi) \quad \text{in } D \times \Omega, \tag{2.2}$$

where $f \in L^2(L^2(D), \Omega)$ is the random source term, ρ and c is density and heat capacity. The initial and boudary condition can be given by $T(x,\xi) = T_0$. In this paper, the static heat transfer problems will be considered, the similar results can be derived with the same procedure for the general cases. Returning to Eq. (2.2), Fourier's law is to eliminate the heat flux, which results in

$$-div\left(\kappa(x,\xi)\nabla T^\varepsilon(x,\xi)\right) = f(x,\xi) \quad \text{in } D \times \Omega. \tag{2.3}$$

2.2 Multi-modes expansion

Referring to [17], the random conductivity $\kappa(x,\xi)$ can be decomposed to two parts, namely

$$\kappa(x,\xi) := \kappa_0(x) + \varepsilon \kappa_1(x,\xi), \tag{2.4}$$

where $\kappa_0(x) \in L^\infty(D)$ is the deterministic coefficients with multiscale characteristics, $\kappa_1(x,\xi)$ is the random fluctuation and ε represents the magnitude of the random fluctuation. Then, some assumptions will be given as follows

(1) For all $\xi \in \Omega$, the conduction coefficient $\kappa(x,\xi)$ satisfies

$$\min_{x \in \overline{D}} \kappa(x,\xi) > \underline{\kappa}$$

for some positive constant $\underline{\kappa}$;

(2) The coefficient $\kappa_0(x)$ is positive and uniformly bounded, that is, there exist positive constants $\underline{\kappa_0}$ and $\overline{\kappa_0}$, such that

$$\underline{\kappa_0} \leq \kappa_0(x) \leq \overline{\kappa_0}, \quad \forall x \in D;$$

(3) For a positive constant $\overline{\kappa_1} > 0$, the $\kappa_1(x,\xi) \in L^2(W^{1,\infty}(D),\Omega)$ satisfies

$$\|\kappa_1(x,\xi)\|_{W^{1,\infty}(D)} \leq \overline{\kappa_1}, \quad \forall \xi \in \Omega, \tag{2.5}$$

where

$$\|T\|_{W^{1,\infty}(D)} := \|T\|_{L^\infty(D)} + \|\nabla T\|_{L^\infty(D)},$$

and the Sobolev space

$$W^{1,\infty}(D) := \{T \in L^\infty(D) : \|T\|_{W^{1,\infty}(D)} < \infty\}.$$

Here, $L^\infty(D)$ is the set of bounded measurable functions equipped with the following norm

$$\|T\|_{L^\infty(D)} := \operatorname*{esssup}_{x \in D} |T(x)|. \tag{2.6}$$

Let $L^2(D)$ be the Hilbert space of all square integrable functions. Then, L^2 inner product is defined by

$$(T,v)_D = \int_D Tv dx, \quad \forall T,v \in L^2(D), \tag{2.7}$$

and the corresponding L^2 norm is given as

$$\|T\|_{L^2(D)}^2 := \int_D |T(x)|^2 dx. \tag{2.8}$$

Let $L^2(\sharp,\Omega)$ denote the space of all measurable function $T : D \times \Omega \to \mathbb{R}$ such that

$$\|T\|_{L^2(\sharp,\Omega)} = \left(\int_\Omega \|T(x,\xi)\|_\sharp^2 dP(\xi) \right)^{\frac{1}{2}} < \infty, \tag{2.9}$$

where $\sharp$ can be taken as $L^2(D)$, $H^1(D)$ or $H_0^1(D)$.

Let $\mathbb{E}(T)$ denotes the expectation defined in the probability space $(\Omega,\mathcal{F},\mathbb{P})$, which is given by:

$$\mathbb{E}(T) := \int_\Omega T(\xi) dP(\xi). \tag{2.10}$$

Then, the corresponding variational form of the problems (2.3) is given as

$$\int_\Omega \left(\kappa \nabla T^\varepsilon, \nabla v \right)_D dP = \int_\Omega (f,v)_D dP, \quad \forall v \in L^2(H_0^1(D),\Omega). \tag{2.11}$$

Assume that T^ε has the following multimodal expansion

$$T^\varepsilon(x,\xi) = \sum_{n=0}^{\infty} \varepsilon^n T_n(x,\xi), \tag{2.12}$$

where $\{T_n\}_{n \geq 0}$ are mode functions. Substituting Eq. (2.12) and Eq. (2.4) into Eq. (2.3), and matching the coefficient of ε^n order terms, the following equations for $\{T_n\}_{n \geq 0}$ can be obtained by

$$\begin{cases} -div\left(\kappa_0(x)\nabla T_0(x,\xi)\right) = f(x,\xi) & \text{in } D \times \Omega, \\ -div\left(\kappa_0(x)\nabla T_n(x,\xi)\right) = div\left(\kappa_1(x,\xi)\nabla T_{n-1}(x,\xi)\right) & \text{in } D \times \Omega \quad \text{for } n \geq 1. \end{cases} \tag{2.13}$$

Furthermore, the boundary conditions for each mode function $\{T_n\}_{n \geq 0}$ is given by

$$T_n(x,\xi) = 0 \quad \text{on } \partial D \quad \text{for } n \geq 0. \tag{2.14}$$

From Eq. (2.13), it is not difficult to find that the mode functions $\{T_n\}_{n \geq 0}$ satisfy a family of heat transfer equations, which have the same deterministic forms in left sides and similar boundary conditions. Especially, the only differences are the random source terms in the right sides, which have a recursive relation for the modal function T_n defined by the previous mode function T_{n-1}. Under approximation of the finite terms, these important features will greatly alleviate the computational cost of randomness, that is

$$T_N^\varepsilon(x,\xi) = \sum_{n=0}^{N-1} \varepsilon^n T_n(x,\xi). \tag{2.15}$$

Moreover, considering multiscale properties of the mode functions $\{T_n\}_{n \geq 0}$, how to efficiently compute the mode functions in multiscale physical space is another challenge. A natural and inexpensive approach is to solve Eqs. (2.13) by multiscale method, which is easily implemented and highly efficient.

2.3 Multiscale formulae of MCEM-GMsFEM

In this subsection, an effective multiscale formulae and algorithm of MCEM-GMsFEM is designed to solve the heat transfer problem (2.3) with uncertain thermal conductivity. Based on the multimode expansion of the solution of problems (2.3) and its finite terms approximation (2.15), CEM-GMsFEM is implemented to solve the multiscale equations governing each mode functions. Then, the Monte Carlo method is used to obtain the expectation of the solution in the probability space, and the detailed algorithm is given.
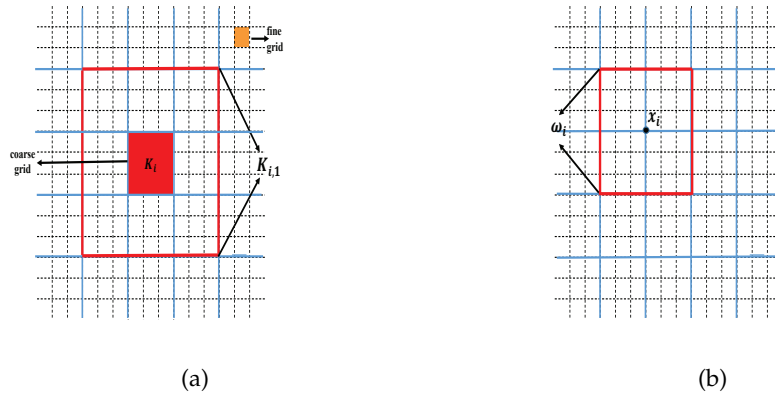
(a)

(b)

Figure 1: The fine grid, coarse grid K_i, oversampling domain $K_{i,1}$, and neighborhood ω_i of the node x_i.

Suppose the domain D (Fig. 1) is composed of a family of meshes $\mathcal{T}^H$, where

$$H = \max_{K_i \in \mathcal{T}^H} H_{K_i}$$

is the coarse mesh size and H_{K_i} is the diameter of coarse grid K_i. $\mathcal{T}^H$ is the uniformly partition of D, and is shape regular. N denotes the number of elements in $\mathcal{T}^H$. And N_c denotes the number of vertices of all coarse grid. Let $\{x_i\}_{i=1}^{N_c}$ be the set of vertices in $\mathcal{T}^H$ and

$$\omega_i = \bigcup \{K_j \in \mathcal{T}^H | x_i \in \overline{K_j}\}$$

be the neighborhood of the node x_i. For each coarse block K_i, the oversampling region $K_{i,m} \subset D$ is defined by enlarging K_i with several coarse grid layers. $\mathcal{T}^h$ is a uniformly refinement of $\mathcal{T}^H$, and h is the diameter of fine grid. Fig. 1 depicts the fine grid, the coarse grid K_i, the oversampling domain $K_{i,1}$ and the neighbor domain ω_i of the node x_i. The construction procedure of multiscale basis functions of CEM-GMsFEM can be divided two steps. Firstly, the auxiliary multiscale space can be obtained by solving a family of local spectral problems. Let $V(K_i) = H^1(K_i)$ for a coarse block K_i, and eigenpairs $\{\lambda_j^{(i)}, \phi_j^{(i)}\} \in \mathbb{R} \times V(K_i)$ satisfy

$$a_i(\phi_j^{(i)}, v) = \lambda_j^{(i)} s_i(\phi_j^{(i)}, v), \quad \forall v \in V(K_i), \tag{2.16}$$

where

$$a_i(u, v) = \int_{K_i} \kappa \nabla u \nabla v dx, \quad s_i(u, v) = \int_{K_i} \tilde{\kappa} uv dx, \tag{2.17}$$

and

$$\tilde{\kappa} = \kappa \sum_{j=1}^{N_c} |\nabla \omega_j|^2,$$

$\{\varpi_j\}$ is a set of partition of unity function in the coarse partition. Assume that the eigen-functions satisfy the normalized condition $s_i(\phi_j^{(i)}, \phi_j^{(i)}) = 1$, and let $\lambda_j^{(i)}$ be arranged in ascending order. The local auxiliary multiscale space can be defined as

$$V_{aux}^{(i)} = \text{span}\{\phi_j^{(i)} | 1 \le j \le L_i\}. \tag{2.18}$$

Then, the global auxiliary space V_{aux} will be assembled from the all local auxiliary space $V_{aux}^{(i)}$.

Secondly, based on the global auxiliary space, the multiscale basis function $\psi_{j,ms}^{(i)} \in H_0^1(K_{i,m})$ will be constructed by energy minimization problem with some constraints as follows

$$\psi_{j,ms}^{(i)} = \text{argmin}\{a(\psi,\psi) | \psi \in H_0^1(K_{i,m}), \ \psi \text{ is } \phi_j^{(i)}\text{-orthogonal}\}, \tag{2.19}$$

where $\phi_j^{(i)}$-orthogonal is defined as

$$s(\psi, \phi_j^{(i)}) = 1, \quad s(\psi, \phi_{j'}^{(i')}) = 0, \quad \text{if } j' \ne j \quad \text{or} \quad i' \ne i. \tag{2.20}$$

Here,

$$s(u,v) = \sum_{i=1}^{N} s_i(u,v), \quad \phi_j^{(i)} \in V_{aux} \quad \text{and} \quad \psi \in H_0^1(D).$$

Then, the multiscale space V_{ms} can be defined as

$$V_{ms} = \text{span}\{\psi_{j,ms}^{(i)} | 1 \le j \le L_i, \ 1 \le i \le N\} \subset H_0^1(D). \tag{2.21}$$

Based on the Eq. (2.13), for each sample ξ_j $(j=1,2,\cdots,M)$ with i.i.d., the multiscale mode functions $\{T_n^{ms}\}_{n\ge0}$ satisfy the following variational problems:

$$\begin{cases} (\kappa_0(x)\nabla T_0^{ms}(x,\xi_j), \nabla v^{ms})_D = (f(x,\xi_j), v^{ms})_D, & \forall v^{ms} \in V_{ms}, \\ (\kappa_0(x)\nabla T_n^{ms}(x,\xi_j), \nabla v^{ms})_D = (\kappa_1(x,\xi_j)\nabla T_{n-1}^{ms}(x,\xi_j), \nabla v^{ms})_D, & \forall v^{ms} \in V_{ms} \text{ for } n \ge 1. \end{cases} \tag{2.22}$$

Suppose $\{T_n^{ms}\}_{n\ge0}$ has the following formulations

$$T_n^{ms}(x,\xi_j) = \sum_{k=1}^{Nc} y_k^n(\xi_j)\psi_{k,ms}(x), \quad \psi_{k,ms}(x) \in V_{ms}. \tag{2.23}$$

Then, Eq. (2.22) can be rewritten the following matrix form

$$\begin{cases} AY^0(\xi_j) = F(\xi_j), \\ AY^n(\xi_j) = G(\xi_j)Y^{n-1}(\xi_j), \end{cases} \tag{2.24}$$

where

$$A = (a_{lq}) \in \mathbb{R}^{Nc \times Nc}, \qquad G(\xi_j) = (g(\xi_j)_{lq}) \in \mathbb{R}^{Nc \times Nc},$$
$$F = (f_q) \in \mathbb{R}^{Nc}, \qquad\qquad Y^n \in \mathbb{R}^{Nc},$$

and

$$a_{lq} = \int_D \kappa_0 \nabla \psi_{l,ms}(x) \nabla \psi_{q,ms}(x) dx, \quad g(\xi_j)_{lq} = \int_D \kappa_1(x,\xi_j) \nabla \psi_{l,ms}(x) \nabla \psi_{q,ms}(x) dx, \quad \text{(2.25a)}$$

$$f_q(\xi_j) = \int_D f(x,\xi_j) \psi_{q,ms}(x) dx, \qquad \boldsymbol{Y}^n(\xi_j) = \left[y_1^n, y_2^n, \cdots, y_{Nc}^n\right]^T, \quad n \geq 1, \qquad \text{(2.25b)}$$

for all $l = 1, 2, \cdots, Nc$, $q = 1, 2, \cdots, Nc$, and $\{\psi_{i,ms}(x)\}_{i=1}^{Nc} \in V_{ms}$. Then, the expectation $\mathbb{E}(T_n)$ for each mode function T_n is given by

$$\mathbb{E}(T_n) = \frac{1}{M} \sum_{j=1}^{M} T_n^{ms}(x, \xi_j). \qquad \text{(2.26)}$$

From Eq. (2.15), the expectation $\mathbb{E}(T^\varepsilon)$ can be approximated by finite truncated terms

$$S_M T_N^{ms} = \sum_{n=0}^{N-1} \varepsilon^n \mathbb{E}(T_n) = \frac{1}{M} \sum_{j=1}^{M} \sum_{n=0}^{N-1} \varepsilon^n T_n^{ms}(x, \xi_j), \qquad \text{(2.27)}$$

and the algorithm is summarized in Algorithm 1.

Algorithm 1: Computation procedure of MCEM-GMsFEM.

Input: $f, \kappa_1, \varepsilon, H, M, N$
Output: $S_M T_N^{ms}(x)$
Set $S_M T_N^{ms}(x) = 0$ (initializing);
Generate the stiffness matrix A on $V_{ms} \times V_{ms}$;
Compute and store the LU decomposition of A;
for $j = 1, 2, \cdots, M$ **do**
    Obtain realizations $\kappa_1(x, \xi_j)$ and $f(x, \xi_j)$;
    Initialization $T_N^{ms}(x, \xi_j) = 0$;
    Compute $\boldsymbol{Y}^0(\xi_j)$ by the LU decomposition of A;
    $A\boldsymbol{Y}^0(\xi_j) = \boldsymbol{F}(\xi_j)$;
    Set $T_N^{ms}(x, \xi_j) \longleftarrow T_N^{ms}(x, \xi_j) + \boldsymbol{Y}^0(\xi_j)$;
    for $n = 1, 2, \cdots, N-1$ **do**
        Compute $\boldsymbol{Y}^n(\xi_j)$ by the LU decomposition of A;
        $A\boldsymbol{Y}^n(\xi_j) = \boldsymbol{G}(\xi_j)\boldsymbol{Y}^{n-1}(\xi_j)$;
        Set $T_N^{ms}(x, \xi_j) \longleftarrow T_N^{ms}(x, \xi_j) + \varepsilon^n \boldsymbol{Y}^n(\xi_j)$;
    end
    Set $S_M T_N^{ms}(x) \longleftarrow S_M T_N^{ms}(x) + \frac{1}{M} T_N^{ms}(x, \xi_j)$.
end

---

3   Convergence analysis

To derive the convergence and error estimates for the finite truncation of multi-modes representation of T^ε, the following Lemma is given.

Lemma 3.1. *Let mode functions $T_n \in L^2(H_0^1(D), \Omega)$ be the solutions of problems* (2.13), *if $f \in L^2(L^2(D), \Omega)$, there holds*

$$\mathbb{E}\|\nabla T_n\|_{L^2(D)} \le C \frac{1}{\underline{\kappa_0}} \left(\frac{\overline{\kappa_1}}{\underline{\kappa_0}} \right)^n \mathbb{E}\|f\|_{L^2(D)}, \quad \forall n \ge 0. \tag{3.1}$$

Proof. With the help of the Lax-Milgram theorem and the elliptic regularity condition [48], the following estimation can be given

$$\mathbb{E}\|\nabla T_0\|_{L^2(D)} \le C \frac{1}{\underline{\kappa_0}} \mathbb{E}\|f\|_{L^2(D)}, \tag{3.2}$$

where the constant C is independent of n and ε.

Moreover, the variation formulations of the second equations of problem (2.13) can be written as

$$\left(\kappa_0 \nabla T_n, \nabla v \right)_D = \left(-\kappa_1 \nabla T_{n-1}, \nabla v \right)_D. \tag{3.3}$$

Let $v = T_n$ and based on Cauchy-Schwarz inequality, we have

$$\underline{\kappa_0} \|\nabla T_n\|_{L^2(D)}^2 \le \left(\kappa_0 \nabla T_n, \nabla T_n \right)_D = \left(-\kappa_1 \nabla T_{n-1}, \nabla T_n \right)_D$$
$$\le \left| \kappa_1 \left(\nabla T_{n-1}, \nabla T_n \right)_D \right| \le \overline{\kappa_1} \|\nabla T_{n-1}\|_{L^2(D)} \|\nabla T_n\|_{L^2(D)}. \tag{3.4}$$

Then, dividing both sides of Eq. (3.4) by $\|\nabla T_{n-1}\|_{L^2(D)}$ and taking the expectation, we have

$$\mathbb{E}\|\nabla T_n\|_{L^2(D)} \le \frac{\overline{\kappa_1}}{\underline{\kappa_0}} \mathbb{E}\|\nabla T_{n-1}\|_{L^2(D)}. \tag{3.5}$$

Applying Eq. (3.5) n times, we get

$$\mathbb{E}\|\nabla T_n\|_{L^2(D)} \le \left(\frac{\overline{\kappa_1}}{\underline{\kappa_0}} \right)^n \mathbb{E}\|\nabla T_0\|_{L^2(D)}. \tag{3.6}$$

Combining with Eq. (3.2), we have

$$\mathbb{E}\|\nabla T_n\|_{L^2(D)} \le C \frac{1}{\underline{\kappa_0}} \left(\frac{\overline{\kappa_1}}{\underline{\kappa_0}} \right)^n \mathbb{E}\|f\|_{L^2(D)}. \tag{3.7}$$

This proof is completed.   □

From above Lemma, the convergence of the multi-modes expansion of the solution in (2.3) can be obtained by the following theorem.

Theorem 3.1. *Let T_N^ε be defined in Eq.* (2.15), *there holds*

$$\lim_{N\to\infty} T_N^\varepsilon = T^\varepsilon \quad in \ \ L^2(H_0^1(D),\Omega). \tag{3.8}$$

Proof. For any fixed positive integer p, we have

$$T_{N+p}^\varepsilon - T_N^\varepsilon = \sum_{n=N}^{N+p-1} \varepsilon^n T_n. \tag{3.9}$$

With the help of Cauchy-Schwarz inequality and Lemma 3.1, we have

$$\mathbb{E}\big[\|\nabla T_{N+p}^\varepsilon - \nabla T_N^\varepsilon\|_{L^2(D)}^2\big] \leq p \sum_{n=N}^{N+p-1} \varepsilon^{2n} \mathbb{E}\|\nabla T_n\|_{L^2(D)}^2$$

$$\leq p \frac{\varepsilon^{2N}(1-\varepsilon^{2p})}{1-\varepsilon^2} \mathbb{E}\|\nabla T_n\|_{L^2(D)}^2 = C(\varepsilon,N,p)\mathbb{E}\|f\|_{L^2(D)}^2, \tag{3.10}$$

where

$$C(\varepsilon,N,p) = C\frac{\overline{\kappa_1}^n}{\underline{k_0}^{n+1}} p \frac{\varepsilon^{2N}(1-\varepsilon^{2p})}{1-\varepsilon^2}. \tag{3.11}$$

Thus, for $\varepsilon < 1$, there exists

$$\lim_{N\to\infty} \mathbb{E}\big[\|\nabla T_{N+p}^\varepsilon - \nabla T_N^\varepsilon\|_{L^2(D)}\big] = 0. \tag{3.12}$$

Here, $\{T_N^\varepsilon\}$ is the Cauchy sequences in Banach space $L^2(H_0^1(D),\Omega)$, and there exists a function $U^\varepsilon \in L^2(H_0^1(D),\Omega)$ satisfies

$$\lim_{N\to\infty} T_N^\varepsilon = U^\varepsilon \quad in \ \ L^2(H_0^1(D),\Omega). \tag{3.13}$$

By the definition of T_N^ε, it is not difficult to find that T_N^ε satisfies

$$\int_\Omega \big(\kappa\nabla T_N^\varepsilon, \nabla v\big)_D dP$$
$$= \int_\Omega (f,v)_D dP + \int_\Omega \varepsilon\kappa_1\big(\nabla(-\varepsilon^{N-1}T_{N-1}),\nabla v\big)_D dP, \quad \forall v\in L^2(H_0^1(D),\Omega). \tag{3.14}$$

Based on Eq. (3.14), we have

$$\left|\int_\Omega \varepsilon^N \kappa_1 \big(\nabla T_{N-1},\nabla v\big)_D dP\right|$$
$$\leq \varepsilon^N|\overline{\kappa_1}|\left|\int_\Omega \big(\nabla T_{N-1},\nabla v\big)_D dP\right|$$
$$\leq \varepsilon^N|\overline{\kappa_1}|\|\nabla T_{N-1}\|_{L^2(D)}\|\nabla v\|_{L^2(D)} \to 0, \tag{3.15}$$

for $N \to \infty$ and $\varepsilon < 1$. Then, from Eq. (3.15), we have

$$\int_{\Omega} \left(\kappa \nabla T_N^{\varepsilon}, \nabla v \right)_D dP = \int_{\Omega} (f, v)_D dP, \quad N \to \infty. \tag{3.16}$$

Thus, U^{ε} is a solution to problem (2.3). By the uniqueness of the solution, we conclude that

$$\lim_{N \to \infty} T_N^{\varepsilon} = T^{\varepsilon}.$$

That is to say the multimodal expansion (2.12) holds in $L^2(H_0^1(D), \Omega)$. This proof is completed. $\qquad\square$

Then, the convergence rate of T_N^{ε} is given in the following theroem.

Theorem 3.2. *Let $T^{\varepsilon} \in L^2(H_0^1(D), \Omega)$ be the solution of problem (2.3), and T_N^{ε} is defined in Eq. (2.15), there holds*

$$\mathbb{E} \| \nabla T^{\varepsilon} - \nabla T_N^{\varepsilon} \|_{L^2(D)} \le C_1 \varepsilon^N \mathbb{E} \| f \|_{L^2(D)}, \tag{3.17}$$

where the constant

$$C_1 = C \frac{\overline{\kappa_1}^N}{\underline{\kappa} \underline{\kappa_0}^N}$$

is independent of ε and the coarse mesh size H.

Proof. For T^{ε} and T_N^{ε}, we have

$$\int_{\Omega} \left(\kappa \nabla T^{\varepsilon}, \nabla v \right)_D dP = \int_{\Omega} (f, v)_D dP, \quad \forall v \in L^2(H_0^1(D), \Omega), \tag{3.18}$$

and

$$\int_{\Omega} \left(\kappa \nabla T_N^{\varepsilon}, \nabla v \right)_D dP$$
$$= \int_{\Omega} (f, v)_D dP - \int_{\Omega} \varepsilon \kappa_1 \left(\nabla \varepsilon^{N-1} T_{N-1}, \nabla v \right)_D dP, \quad \forall v \in L^2(H_0^1(D), \Omega). \tag{3.19}$$

Subtracting Eq. (3.19) from Eq. (3.18) yields

$$\int_{\Omega} \left(\kappa \nabla (T^{\varepsilon} - T_N^{\varepsilon}), \nabla v \right)_D dP = \int_{\Omega} \varepsilon \kappa_1 \left(\nabla \varepsilon^{N-1} T_{N-1}, \nabla v \right)_D dP. \tag{3.20}$$

Then, define $R_N^{\varepsilon} = T^{\varepsilon} - T_N^{\varepsilon}$ and let $v = R_N^{\varepsilon}$, we have

$$\begin{aligned}
\underline{\kappa} \| \nabla R_N^{\varepsilon} \|_{L^2(D)}^2 &\le \left(\kappa \nabla R_N^{\varepsilon}, \nabla R_N^{\varepsilon} \right)_D \\
&\le \varepsilon^N \kappa_1 \| \nabla T_{N-1} \|_{L^2(D)} \| \nabla R_N^{\varepsilon} \|_{L^2(D)} \\
&\le \varepsilon^N \overline{\kappa_1} \| \nabla T_{N-1} \|_{L^2(D)} \| \nabla R_N^{\varepsilon} \|_{L^2(D)}.
\end{aligned} \tag{3.21}$$

Combining with Lemma 3.1, we have

$$\mathbb{E} \| \nabla R_N^{\varepsilon} \|_{L^2(D)} \le C \frac{(\varepsilon \overline{\kappa_1})^N}{\underline{\kappa} \underline{\kappa_0}^N} \mathbb{E} \| f \|_{L^2(D)}.$$

This completes the proof. $\qquad\square$

Similar to the Lemma 3.1, the mode functions $\{T_n^{ms}\}_{n\geq 0}$ satisfy the following Lemma.

Lemma 3.2. *Let $T_n^{ms}\in L^2(H_0^1(D),\Omega)$ be the solutions of problems (2.22), if $f\in L^2(L^2(D),\Omega)$, there holds*

$$\mathbb{E}\|\nabla T_n^{ms}\|_{L^2(D)}\leq C\frac{1}{\underline{\kappa_0}}\left(\frac{\overline{\kappa_1}}{\underline{\kappa_0}}\right)^n\mathbb{E}\|f\|_{L^2(D)},\quad\forall n\geq 0. \tag{3.22}$$

Next, the error estimates of MCEM-GMsFEM will be given in next theorem.

Theorem 3.3. *Let mode functions T_n and T_n^{ms} be the solutions of problems (2.13) and (2.22), there holds*

$$\mathbb{E}\|\kappa_0\left(\nabla T_N^\varepsilon-\nabla T_N^{ms}\right)\|_{L^2(D)}\leq C_2(\varepsilon,N)H\Lambda^{-\frac{1}{2}}\mathbb{E}\|f\|_{L^2(D)}, \tag{3.23}$$

where the constant $C_2(\varepsilon,N)$ is independent of κ_0, and the coarse mesh size H.

Proof. The definition of T_N^ε and T_N^{ms} are shown as follows

$$T_N^\varepsilon=\sum_{n=0}^{N-1}\varepsilon^n T_n,\quad T_N^{ms}=\sum_{n=0}^{N-1}\varepsilon^n T_n^{ms}. \tag{3.24}$$

In order to estimate $\mathbb{E}\|\kappa_0(\nabla T_N^\varepsilon-\nabla T_N^{ms})\|_{L^2(D)}$, we need consider $T_n-T_n^{ms}$. For each mode function T_n, define auxiliary function $\widehat{T}_n\in V_{ms}$ as the solution of the following variational form

$$\left(\kappa_0\nabla\widehat{T}_n(x,\xi_j),\nabla v\right)_D=\left(-\kappa_1(x,\xi_j)\nabla T_{n-1}(x,\xi_j),\nabla v\right)_D,\quad\forall v\in V_{ms},\quad\text{and}\quad\forall n\geq 1. \tag{3.25}$$

Then, for each fixed sample ξ_j, $T_n-T_n^{ms}$ can be written as

$$T_n-T_n^{ms}=T_n-\widehat{T}_n+\widehat{T}_n-T_n^{ms}.$$

By use of Lemma 1 in [33], we have

$$\begin{aligned}\|\kappa_0\left(\nabla T_n-\nabla\widehat{T}_n\right)\|_{L^2(D)}&\leq CH\Lambda^{-\frac{1}{2}}\|\kappa_0^{-\frac{1}{2}}\left(-\kappa_1\nabla T_{n-1}\right)\|_{L^2(D)}\\&\leq CH\Lambda^{-\frac{1}{2}}\underline{\kappa_0}^{-\frac{1}{2}}\overline{\kappa_1}\|\nabla T_{n-1}\|_{L^2(D)}.\end{aligned} \tag{3.26}$$

From Lemma 3.1, we deduce

$$\mathbb{E}\|\kappa_0\left(\nabla T_n-\nabla\widehat{T}_n\right)\|_{L^2(D)}\leq CH\Lambda^{-\frac{1}{2}}\frac{\overline{\kappa_1}^n}{\underline{\kappa_0}^{n+\frac{1}{2}}}\mathbb{E}\|f\|_{L^2(D)}. \tag{3.27}$$

Moreover, for $\{T_n^{ms}\}_{n\geq 1}\in V_{ms}$, we get

$$\left(\kappa_0\nabla T_n^{ms}(x,\xi_j),\nabla v\right)_D=\left(-\kappa_1(x,\xi_j)\nabla T_{n-1}^{ms}(x,\xi_j),\nabla v\right)_D,\quad\forall v\in V_{ms}. \tag{3.28}$$

For any sample ξ_j, combining Eq. (3.25) with Eq. (3.28), it follows that

$$\left(\kappa_0(\nabla\widehat{T}_n - \nabla T_n^{ms}), \nabla v\right)_D = \left(-\kappa_1(\nabla T_{n-1} - \nabla T_{n-1}^{ms}), \nabla v\right)_D, \quad \forall v \in V_{ms}. \tag{3.29}$$

Let

$$v = \widehat{T}_n - T_n^{ms} \in V_{ms},$$

based on Cauchy-Schwarz inequality and Lemma 3.2, there exists

$$\mathbb{E}\|\kappa_0(\nabla\widehat{T}_n - \nabla T_n^{ms})\|_{L^2(D)} \leq \overline{\kappa_1}\mathbb{E}\|\nabla T_{n-1} - \nabla T_{n-1}^{ms}\|_{L^2(D)}. \tag{3.30}$$

Under the relation of Eq. (3.30), we have

$$\mathbb{E}\|\kappa_0(\nabla\widehat{T}_n - \nabla T_n^{ms})\|_{L^2(D)} \leq \overline{\kappa_1}^n \mathbb{E}\|\nabla T_0 - \nabla T_0^{ms}\|_{L^2(D)}. \tag{3.31}$$

Combining (3.27) with (3.31), the following estimation is given

$$\begin{aligned}
&\mathbb{E}\|\kappa_0(\nabla T_N^\varepsilon - \nabla T_N^{ms})\|_{L^2(D)} \\
&\leq \sum_{n=0}^{N-1} \varepsilon^n \left(\mathbb{E}\|\kappa_0(\nabla T_n - \nabla\widehat{T}_n)\|_{L^2(D)} + \mathbb{E}\|\kappa_0(\nabla\widehat{T}_n - \nabla T_n^{ms})\|_{L^2(D)}\right) \\
&\leq CH\Lambda^{-\frac{1}{2}} \frac{\overline{\kappa_1}^n}{\underline{\kappa_0}^{n+\frac{1}{2}}} \sum_{n=0}^{N-1} \varepsilon^n \mathbb{E}\|f\|_{L^2(D)} + \overline{\kappa_1}^n \mathbb{E}\|\nabla T_0 - \nabla T_0^{ms}\|_{L^2(D)} \\
&\leq C_2(\varepsilon, N) H\Lambda^{-\frac{1}{2}} \mathbb{E}\|f\|_{L^2(D)},
\end{aligned} \tag{3.32}$$

where

$$C_2(\varepsilon, N) = C\left(\frac{\overline{\kappa_1}^n}{\underline{\kappa_0}^{n+\frac{1}{2}}}\right) \frac{1-\varepsilon^N}{1-\varepsilon} + C\overline{\kappa_1}^n \mathbb{E}\|\nabla T_0 - \nabla T_0^{ms}\|_{L^2(D)}. \tag{3.33}$$

This completes the proof. □

Then, the statistical error rate for the Monte Carlo method will be given in the next theorem.

Theorem 3.4. *Let $S_M T_N^{ms}$ be defined in Eq. (2.27), there holds*

$$\mathbb{E}\|\mathbb{E}(\nabla T_N^{ms} - \nabla S_M T_N^{ms})\|_{L^2(D)}^2 \leq \frac{C}{M} \frac{1-\varepsilon^{2N}}{1-\varepsilon^2} \left(\frac{1}{\underline{\kappa_0}} \left(\frac{\overline{\kappa_1}}{\underline{\kappa_0}}\right)^n\right)^2 \mathbb{E}\|f\|_{L^2(D)}^2, \tag{3.34}$$

where the constant C is independent of ε and M.

Proof. Define

$$\mathbb{E}(T_N^{ms}) = \sum_{n=0}^{N-1} \varepsilon^n \mathbb{E}(T_n^{ms}), \quad S_M T_N^{ms} = \sum_{n=0}^{N-1} \varepsilon^n \left[\frac{1}{M}\sum_{j=1}^{M} T_n^{ms}(x, \xi_j)\right]. \tag{3.35}$$

From the standard estimations for Monte Carlo method, we have

$$\mathbb{E}\|\nabla\mathbb{E}(T_N^{ms} - \nabla S_M T_N^{ms})\|_{L^2(D)}^2$$

$$\leq 2\sum_{n=0}^{N-1}\varepsilon^{2n}\mathbb{E}\left(\|\nabla(\mathbb{E}(T_n^{ms}) - \frac{1}{M}\sum_{j=1}^{M}T_n^{ms}(x,\xi_j)\|_{L^2(D)}^2\right)$$

$$\leq \frac{2}{M}\sum_{n=0}^{N-1}\varepsilon^{2n}\mathbb{E}(\|\nabla T_n^{ms}\|_{L^2(D)}^2). \tag{3.36}$$

By virtue of Lemma 3.2, it follows that

$$\mathbb{E}\|\nabla\mathbb{E}(T_N^{ms} - \nabla S_M T_N^{ms})\|_{L^2(D)}^2 \leq \frac{C}{M}\frac{1-\varepsilon^{2N}}{1-\varepsilon^2}\left(\frac{1}{\underline{\kappa_0}}\left(\frac{\overline{\kappa_1}}{\underline{\kappa_0}}\right)^n\right)^2\mathbb{E}\|f\|_{L^2(D)}^2. \tag{3.37}$$

This completes the proof. □

Remark 3.1. The error order of standard Monte Carlo method is $\mathcal{O}(M^{\frac{1}{2}})$, a large number of samples will be chosen to improve the accuracy of the numerical results. Some improved version of Monte Carlo method can be used to reduce the computation burden, such as Multilevel Monte Carlo method, Multifielty Monte Carlo method, etc.

Finally, the total error of our proposed MCEM-GMsFEM can be divided three parts as follows

$$\mathbb{E}(T^\varepsilon) - S_M T_N^{ms} = \left(\mathbb{E}(T^\varepsilon) - \mathbb{E}(T_N^\varepsilon)\right) + \left(\mathbb{E}(T_N^\varepsilon) - \mathbb{E}(T_N^{ms})\right) + \left(\mathbb{E}(T_N^{ms}) - S_M T_N^{ms}\right). \tag{3.38}$$

Then, combining (3.17), (3.23) and (3.34), the following error estimate for the full algorithm is given.

Theorem 3.5. *Suppose the source term* $f \in L^2(L^2(D),\Omega)$, *and let* $S_M T_N^{ms}$ *be defined in Eq. (2.27), there holds*

$$\mathbb{E}\|\kappa_0(\nabla\mathbb{E}(T^\varepsilon) - \nabla S_M T_N^{ms})\|_{L^2(D)} \leq C(\varepsilon^N + H + M^{-\frac{1}{2}})\mathbb{E}\|f\|_{L^2(D)}, \tag{3.39}$$

where the positive constant C is independent of ε, *the coarse mesh size H, N and M.*

4   Numerical examples

In this section, some numerical examples are given to verify the efficiency and accuracy of the proposed MCEM-GMsFEM. In the following two examples, the problems (2.3) are considered in the spatial domain $D = [0,1]^2$. The solutions $S_M T_N^{ms}$ of MCEM-GMsFEM will be compared with the reference solutions $\mathbb{E}(T^h)$ and MFEM solutions $S_M T_N^h$. The reference solutions

$$\mathbb{E}(T^h) = \frac{1}{M}\sum_{i=1}^{M}T^h(x,\xi_i)$$

are given by use of stochastic finite element method, where h is fine grid size of uniform partition over D. The solutions of multi-modes finite element method (MFEM) is defined by

$$S_M T_N^h = \frac{1}{M} \sum_{i=1}^{M} \sum_{n=0}^{N-1} \varepsilon^n T_n^h(x, \xi_i),$$

whose gird size is same to the reference solution. The Monte Carlo procedure with $M = 10^3$ samples ξ_i are carried out to compute the mean value. Then, based on Theorem 3.5, the accuracy of the proposed MCEM-GMsFEM is defined by the relative L^2 and energy errors are defined as follows:

$$e_{L^2} = \frac{\|\mathbb{E}(T^h(x,\xi)) - S_M T_N^{ms}(x,\xi)\|_{L^2(D)}}{\|\mathbb{E}(T^h(x,\xi))\|_{L^2(D)}}, \tag{4.1a}$$

$$e_a = \frac{\|\mathbb{E}(T^h(x,\xi)) - S_M T_N^{ms}(x,\xi)\|_a}{\|\mathbb{E}(T^h(x,\xi))\|_a}, \tag{4.1b}$$

where energy norm is defined by

$$\|u\|_a^2 := \int_D \kappa_0(x) |\nabla u(x)|^2 dx. \tag{4.2}$$

4.1 Validation of the theoretical results

In this example, some theoretical results for the convergence rate of MCEM-GMsFEM are verified. The thermal conductivity $k_0(x)$ for the numerical tests are depicted in Fig. 2(a) with the contrast ratio 10^4. Then, the fluctuation $\kappa_1(x,\xi)$ and source term $f(x,\xi)$ are defined as

$$\kappa_1(x,\xi) = 0.6 + 0.6 \sum_{i=1}^{M_\eta} \sum_{j=1}^{M_\eta} \exp(-2) \alpha_{i,j}(x) Z_{i,j}^1(\xi), \tag{4.3a}$$

$$f(x,\xi) = \exp(\pi) \sin(2\pi x) \cos(2\pi y) + \sum_{i=1}^{M_f} \sum_{j=1}^{M_f} \exp(ij) \beta_{i,j}(x) Z_{i,j}^2(\xi), \tag{4.3b}$$

where $Z_{i,j}^1(\xi)$, $(i,j = 1,2,\cdots,M_\eta)$ is the uniform distribution in $[0,1]$, and $Z_{i,j}^2(\xi)$, $(i,j = 1,2,\cdots,M_f)$ is the standard Gaussian distribution with i.i.d..

$$\alpha_{i,j}(x) = \sin(ix_1 + jx_2), \quad \beta_{i,j}(x) = \cos(i\pi x_1) \sin(j\pi x_2), \tag{4.4}$$

where $M_\eta = 10$ and $M_f = 5$.

Figs. 2(b)-(d) demonstrate the numerical results of reference solutions $\mathbb{E}(T^h)$, the fininte element solution $S_M T_N^h$ with multimode expantion, and the corresponding MCEM-GMsFEM solutions $S_M T_N^{ms}$, where the coarse mesh size is $H = 1/10$, the truncation number N of multi-modes expansion is fixed to 5, the oversampling layer is $m = 4$, and the
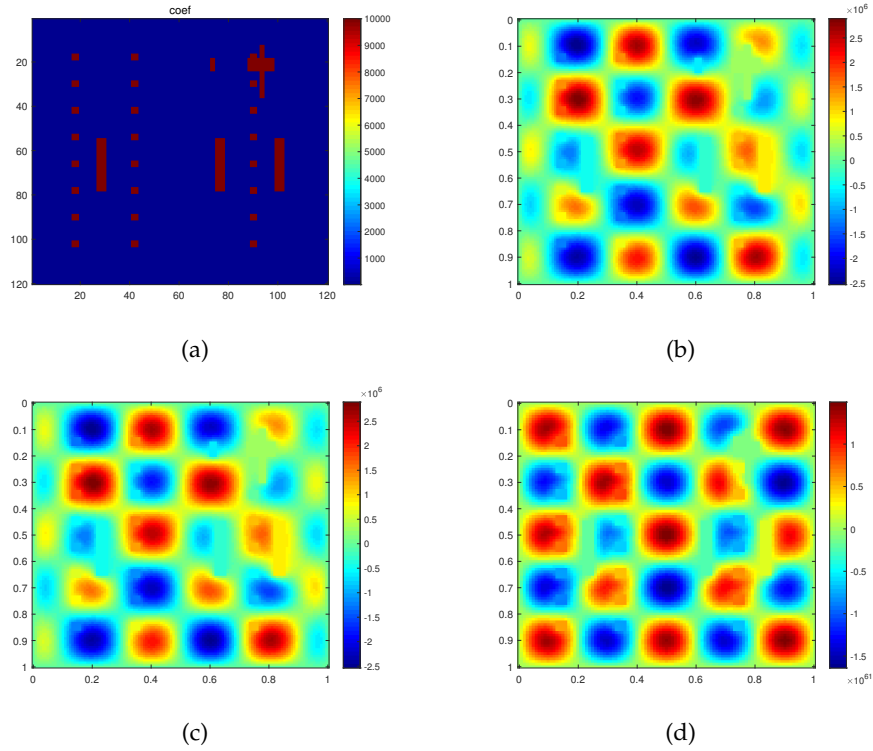
Figure 2: (a) Thermal conductivity $k_0(x)$, (b) the reference solution $\mathbb{E}(T^h)$, (c) MFEM solution $S_M T_5^h$ and (d) MCEM-GMsFEM solution $S_M T_5^{ms}$ computed for $\varepsilon = 0.1$.

number of local multiscale basis functions is chosen as 4. Here, the 120×120 fine grid is used for reference solution, and 10×10 coarse grid for the proposed MCEM-GMsFEM. From above figure, it clearly shows that the difference between MCEM-GMsFEM solution and reference solution is small. In Fig. 3, the cross sections of solutions in Figs. 2(b)-(d) on the line $y = x$ is depicted. It can be found that the proposed MCEM-GMsFEM can efficiently model heat transfer problems with multiscale uncertain material parameters.

Fig. 4 shows the convergence results of MCEM-GMsFEM under different numbers of

Table 1: Relative errors under different coarse grid size H, oversampling layer m with $\varepsilon = 0.1$.

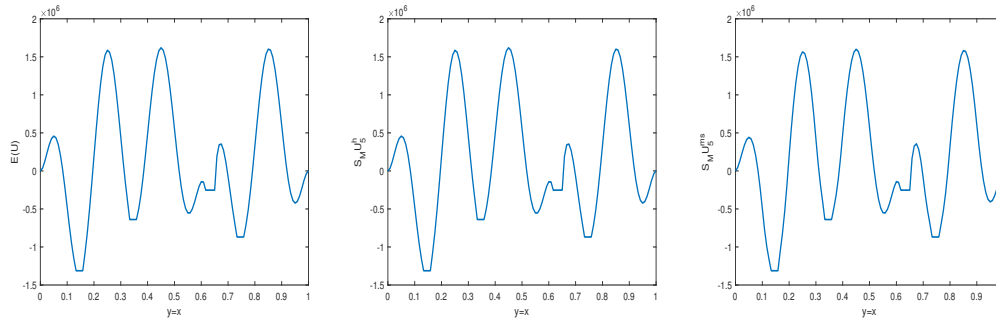| H	Number basis per element	m	N	e_{L2}	e_a
1/5	4	3	5	$2.0087e-01$	$3.6030e-01$
1/6	4	4	5	$1.2885e-01$	$2.6240e-01$
1/8	4	4	5	$8.7953e-01$	$1.9683e-01$
1/10	4	4	5	$1.2708e-02$	$5.5169e-02$
1/12	4	5	5	$1.3205e-02$	$5.3185e-02$

Figure 3: Cross sections of $\mathbb{E}(T^h)$, $S_M T_5^h$ and $S_M T_5^{ms}$ which is plotted in Fig. 2 computed for $\varepsilon = 0.1$, over the line $y = x$.

(a)   (b)
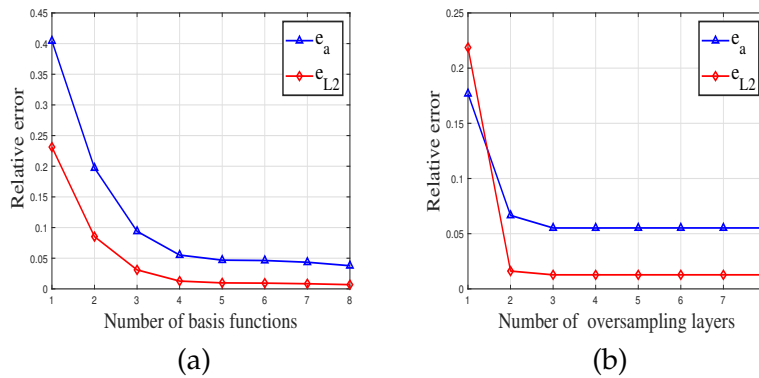
Figure 4: Relative errors under different numbers of local basis functions (a), different numbers of oversampling layers (b).

local multiscale basis functions, oversampling layer m, where the truncation number N of multi-modes expansion is fixed to 5. Some phenomena have been observed that the relative L^2 and energy errors rapidly decay with the numbers of local multiscale basis functions and oversampling layer m increased. Therefore, we will select 4 basis functions for each coarse grid in this example. Then, the influence of the coarse grid size H and the fluctuation ε on the computation accuracy are presented in Tables 1 and 2. The relative error decreases as the coarse grid size H and the fluctuation ε decrease, which is consistent with our theoretical analysis.

Table 2: Relative errors varying with the magnitude of random fluctuation ε where $N = 5$, $H = 1/10$.

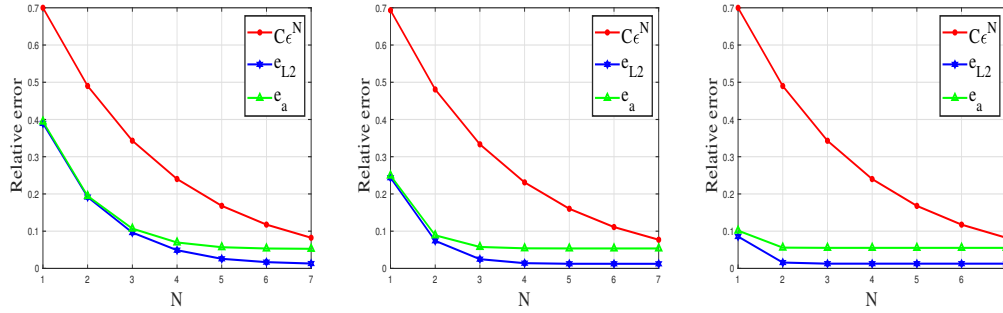| ε	$\varepsilon = 0.9$	$\varepsilon = 0.8$	$\varepsilon = 0.7$	$\varepsilon = 0.5$	$\varepsilon = 0.4$
e_{L2}	$4.0153e{-}01$	$2.2688e{-}01$	$1.1896e{-}01$	$2.5766e{-}02$	$1.4265e{-}02$
e_a	$3.9464e{-}01$	$2.2651e{-}01$	$1.2614e{-}01$	$5.6891e{-}02$	$5.3454e{-}02$

Figure 5: Plots of MCEM-GMsFEM relative errors and $C\varepsilon^N$ with $\varepsilon = 0.5$ (Left), $\varepsilon = 0.3$ (Middle) and $\varepsilon = 0.1$ (Right).

In Fig. 5, the convergence rate of relative L^2 and energy errors between the reference solution $\mathbb{E}(T^\varepsilon)$ and the MCEM-GMsFEM solution $S_M T_N^{ms}$ are demonstrated for the mode number $N = 1, 2, \cdots, 7$. The error converges at a rate $\mathcal{O}(\varepsilon^N)$ as derived in Theorem 3.5. It is easy to find that the relative error rapidly reduces when the number of modal functions increases. Moreover, the relative error can be reduced by use of more mode functions for relatively large ε.

4.2 Application to random fields

In this example, numerical experiment is carried out by use of

$$\kappa_1(\mathbf{x}, \xi) = \exp\left(X(\mathbf{x}, \xi)\right),$$

where random fields $X(\mathbf{x}, \xi)$ in Eq. (2.4) is defined by exponential quadratic kernel as follows

$$\mathcal{K}(\mathbf{x}, \mathbf{x}') = \sigma^2 \exp\left(-\frac{\|\mathbf{x} - \mathbf{x}'\|_2^2}{2 l_\mathbf{x}^2}\right) \tag{4.5}$$

with $\mathbf{x}$ and $\mathbf{x}'$ are spatial coordinates in D, σ^2 is the overall variance (σ is also known as amplitude), $l_\mathbf{x}$ is the length scale. For simplicity, the thermal conductivity are sampled under the help of Karhunen-Loeve expansion (KLE)

$$X(\mathbf{x}, \xi) = \mathbb{E}(X) + \sum_{i=1}^{N_{kl}} \sqrt{\lambda_i} b_i(\mathbf{x}) \xi_i, \tag{4.6}$$

where $\mathbb{E}(X) = 1$, $\sigma = 0.2$, and $l_\mathbf{x} = 0.5$. The random variable ξ_i obeys the standard Gaussian distribution with i.i.d., λ_i and $b_i(\mathbf{x})$ are the corresponding eigenvalues and eigenvectors. Fig. 6(a) depicts the coefficient function $k_0(\mathbf{x})$ with the contrast ratio 10^4, and Figs. 6(b)-(d) give three samples of random fluctuation $k_1(\mathbf{x}, \xi)$ used in this example. The source term $f(\mathbf{x}, \xi)$ is taken as

$$f(\mathbf{x}, \xi) = 6\exp(\mathbf{x})\exp(\xi_1 \xi_2)\cos(\xi_3), \tag{4.7}$$
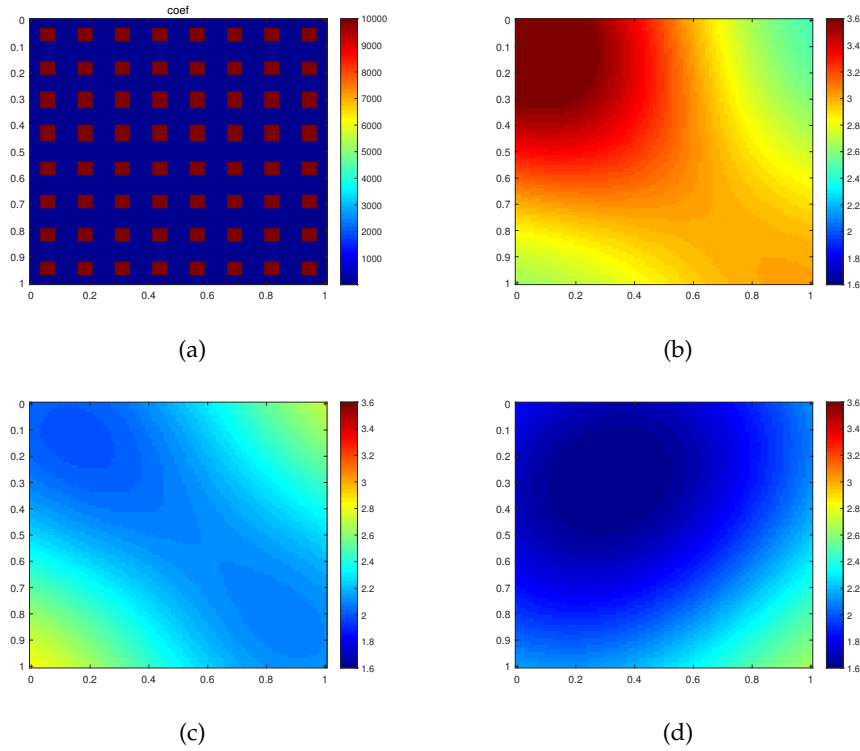
(a)

(b)

(c)

(d)

Figure 6: (a) Thermal conductivity $k_0(x)$, (b)-(d) Three samples generated by random fluctuation $\kappa_1(x,\xi)$.
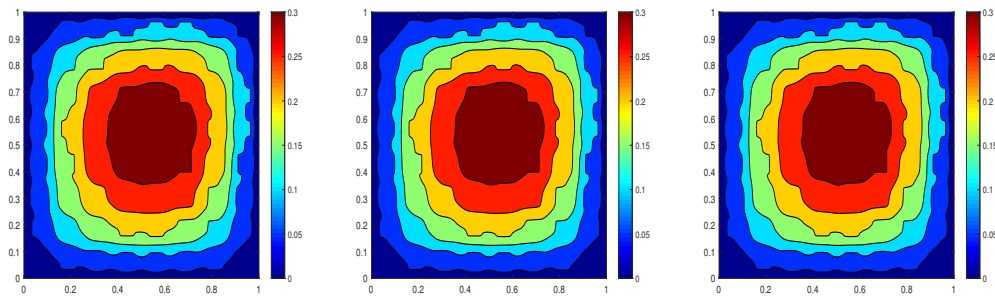

Figure 7: Contour of expectation for the reference solution $\mathbb{E}(T^h)$, MFEM solution $S_M T_5^h$ and MCEM-GMsFEM solution $S_M T_5^{ms}$ with $\varepsilon = 0.1$.

where ξ_i, $(i=1,2,3)$ obey the Beta distribution **B**(1,1).

In Fig. 7, the contours of the reference solution $\mathbb{E}(T^h)$, the MFEM solution $S_M T_N^h$, and MCEM-GMsFEM solution $S_M T_N^{ms}$ are demonstrated with $N=5$, where the reference solution and MFEM solution are defined by the domain D partitioned uniformly with
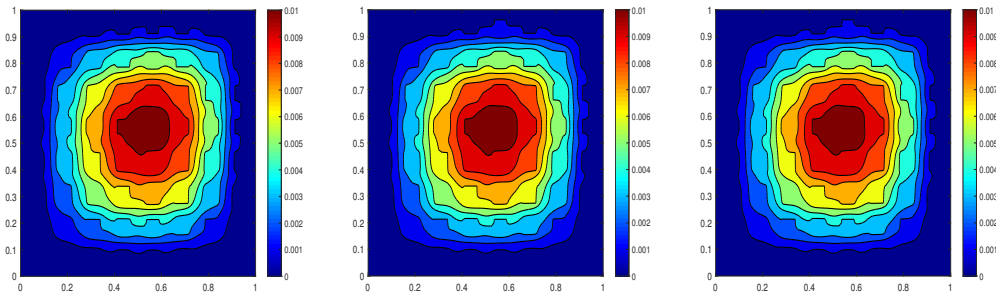
Figure 8: Contour of variance for the reference solution $var(T^h)$, MFEM solution $var(T_5^h)$ and MCEM-GMsFEM solution $var(T_5^{ms})$ with $\varepsilon = 0.1$.
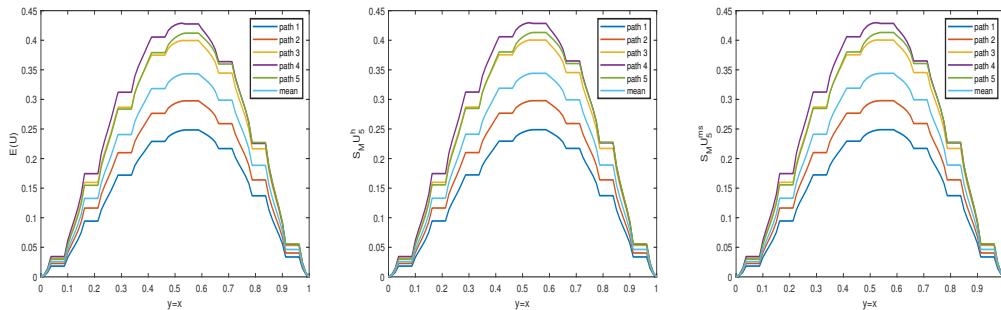

Figure 9: Cross sections of $\mathbb{E}(T^h)$, $S_M T_5^h$ and $S_M T_5^{ms}$ which is plotted in Fig. 7 with $\varepsilon = 0.1$, over the line $y = x$.

$h = 1/80$, and the grid size of MCEM-GMsFEM is taken as $H = 1/8$. The contours of their variance are also drawn in Fig. 8. It is clear that MCEM-GMsFEM produces an accurate approximation in comparison with the standard and multi-modes stochastic finite element method. Fig. 9 plots the first five Monte Carlo sampling paths of the corresponding three solution on $y = x$, and the mean value is shown in color blue, which is consistent with our theoretical results.

In Tables 3 and 4, $\varepsilon = 0.05, 0.1, 0.3, 0.5$ are chosen for comparison under the relative errors e_{L_2} and e_a. We observe that the MCEM-GMsFEM can accurately approximate the

Table 3: Relative errors e_{L2} varying with the magnitude of the random fluctuation ε and N.

ε	$N=3$	$N=4$	$N=5$	$N=6$	$N=7$
0.05	$2.9347e-03$	$1.5614e-03$	$1.3910e-03$	$1.4069e-03$	$1.4041e-03$
0.1	$2.2785e-02$	$7.3888e-03$	$2.2914e-03$	$1.6969e-03$	$1.3728e-03$
0.3	$6.0979e-01$	$5.4790e-01$	$5.0510e-01$	$4.8044e-01$	$4.6912e-01$
0.5	2.7941	4.1654	6.3848	10.0723	16.3549

Table 4: Relative errors e_a varying with the magnitude of the random fluctuation ε and N.

ε	$N=3$	$N=4$	$N=5$	$N=6$	$N=7$
0.05	$2.0184e-02$	$1.9979e-02$	$1.9974e-02$	$1.9974e-02$	$1.9974e-02$
0.1	$3.0585e-02$	$2.1276e-02$	$2.0223e-02$	$2.0120e-02$	$2.0110e-02$
0.3	$6.1017e-01$	$5.4781e-01$	$5.0586e-01$	$4.8085e-01$	$4.7049e-01$
0.5	2.7928	4.1631	6.3841	10.0755	16.3718

reference solution for $\varepsilon=0.05$, 0.1, 0.3 when the mode function number N increase. However, for $\varepsilon=0.5$, it is different to previous examples working for a large ε value, which is similar to the test in Table 2. This is possibly a result of the tests in this example being carried out with a relatively complicated random fluctuation parameter and some ensemble method (see [49]) should be tried to improve the results in further research. In spite of this, the fluctuation ε and mode function number N can be chosen to be relatively small to obtain an accurate approximation, which will lead to great saving in the computation time.

5   Conclusions

The objective of this paper is to design an effective stochastic multiscale method for solving heat transfer problem with uncertain multiscale thermal conductivity, which incorporate the merits of multi-modes method and CEM-GMsFEM. The multi-modes method can transform the original stochastic multiscale problem into a series of recursive multiscale models sharing the same deterministic thermal conductivity by multiscale analysis in random space. With the help of MCEM-GMsFEM and LU decomposition, MCEM-GMsFEM provides an efficient procedure to obtain an approximation to stochastic multiscale systems. The optimal error order is derived in detail, and the efficiency and accuracy of MCEM-GMsFEM are verified by several numerical examples, which are consistent with the theoretical results.

Acknowledgements

References

[1] W. H. NG, P. P. FRIEDMANN, AND A. M. WAAS, *Thermomechanical behavior of a damaged thermal protection system: Finite-element simulations,* J. Aerospace Eng., 25 (2012), pp. 90–102.

[2] L. S. FLETCHER, M. A. LAMBERT, AND E. E. MAROTTA, *Thermal enhancement coatings for microelectronic systems,* J. Electronic Packaging, 120 (1998), pp. 229–237.

[3] H. DONG, J. CUI, Y. NIE, Z. YANG, AND Z. YANG, *Multiscale computational method for heat conduction problems of composite structures with diverse periodic configurations in different subdomains,* Comput. Math. Appl., 76(11) (2018), pp. 2549–2565.

[4] P. MAREPALLI, J. Y. MURTHY, B. QIU, AND X. RUAN, *Quantifying uncertainty in multscale heat conduction calculations,* J. Heat Transf., 136 (2014), pp. 1–10.

[5] S. BOYAVAL, C. L. BRIS, Y. MADAY, N. NGUYEN, AND A. PATERA, *A reduced basis approach for variational problems with stochastic parameters: application to heat conduction with variable robin coefficient,* Comput. Methods Appl. Mech. Eng., 198 (2009), pp. 3187–3206.

[6] M KAMIŃSKI AND P. OSTROWSKI, *Homogenization of heat transfer in fibrous composite with stochastic interface defects,* Compos. Struct., 261 (2021), 113555.

[7] R. CHIBA, *Stochastic analysis of heat conduction and thermal stresses in solids: a review,* Heat Transf. Phenomena Appl., (2012).

[8] D. XIU AND G. E. KARNIADAKIS, *A new stochastic approach to transient heat conduction modeling with uncertainty,* Int. J. Heat Mass Transf., 46(24) (2003), pp. 4681–4693.

[9] S. TORQUATO, Random Heterogeneous Materials: Microstructure and Macroscopic Properties, Springer, 2001.

[10] E. RUSSEL AND CAFLISCH, *Monte carlo and quasi-monte carlo methods,* Acta Numer., 7 (2005), pp. 1–49.

[11] D. DAI, Y. EPSHTEYN, AND A. NARAYAN, *Hyperbolicity-preserving and well-balanced stochastic galerkin method for shallow water equations,* J. Sci. Comput., 43 (2021), pp. A929–A952.

[12] R. PULCH, *Stochastic galerkin methods for analyzing equilibria of random dynamical systems,* J. Uncertainty Quantification, 1 (2013), pp. 408–430.

[13] F. NOBILE, R. TEMPONE, AND C. WEBSTER, *A sparse grid stochastic collocation method for partial differential equations with random input data,* J. Numer. Anal., 46 (2008), pp. 2309–2345.

[14] A. TECKENTRUP, P. JANTSCH, C. WEBSTER, AND M. GUNZBURGER, *A multilevel stochastic collocation method for partial differential equations with random input data,* J. Uncertainty Quantification, 3 (2015), pp. 1046–1074.

[15] I. BABUŠKA, F. NOBILE, AND R. TEMPONE, *A stochastic collocation method for elliptic partial differential equations with random input data,* J. Numer. Anal., 45 (2007), pp. 1005–1034.

[16] X. FENG, J. LIN, AND C. LORTON, *An efficient numerical method for acoustic wave scattering in random media,* J. Uncertainty Quantification, 3 (2015), pp. 790–822.

[17] X. FENG, J. LIN, AND C. LORTON, *A multimodes monte carlo finite element method for elliptic partial differential equations with random coefficients,* Int. J. Uncertainty Quantification, 6 (2016), pp. 429–443.

[18] X. FENG AND C. LORTON, *An efficient monte carlo interior penalty discontinuous Galerkin method for elastic wave scattering in random media,* Comput. Methods Appl. Mech. Eng., 315 (2016), pp. 141–168.

[19] X. FENG, J. LIN, AND C. LORTON, *An efficient monte carlo interior penalty discontinuous Galerkin method for the time-harmonic Maxwell's equations with random coefficients,* J. Sci. Comput., 80 (2019), pp. 1498–1528.

[20] X. FENG, Y. LUO, L. VO, AND Z. WANG, *An efficient iterative method for solving parameter-*

dependent and random convection-diffusion problems, J. Sci. Comput., 90 (2022), 72.

[21] A. BENSOUSSAN, J. L. LIONS, AND G. PAPANICOLAOU, Asymptotic Analysis for Periodic Structures. Elsevier North-Holland, 1978.

[22] A. GRGOIRE AND H. ZAKARIA, *Homogenization of a conductive, convective, and radiative heat transfer problem in a heterogeneous domain,* SIAM J. Math. Anal., 45(3) (2013), pp. 1136–1178.

[23] F. PIOTR, *Heat conduction in composites: Homogenization and macroscopic behavior,* Appl. Mech. Rev., 50(6) (1997), pp. 327–356.

[24] E. SANCHEZ-PALENCIA AND A. C. ZAOUI, Homogenization Technques for Composite Media, Springer-Verlag, 1987.

[25] B. DU, H. SU, AND X. L. FENG, *Two-level variational multiscale method based on the decoupling approach for the natural convection problem,* Int. Commun. Heat Mass Transf., 61 (2015), pp. 128–139.

[26] B. GANAPATHYSUBRAMANIAN AND N. ZABARAS, *Modeling diffusion in random heterogeneous media: Data-driven models, stochastic collocation and the variational multiscale method,* J. Comput. Phys., 226 (2007), pp. 326–353.

[27] T. J. HUGHES, G. R. FEIJO, L. MAZZEI, AND J. B. QUINCY, *The variational multiscale methods paradigm for computational mechanics,* Comput. Methods Appl. Mech. Eng., 166(1) (1998), pp. 3–24

[28] V. JOHN AND S. KAYA, *A finite element variational multiscale method for the Navier–Stokes equations,* J. Sci. Comput., 26 (2005), pp. 1485–1503.

[29] J. EBERHARD, *Upscaling for stationary transport in heterogeneous porous media,* Multiscale Model. Simulation, 3 (2005), pp. 957–976.

[30] F. LIST, K. KUMAR, IULIU S. POP, AND F. RADU, *Rigorous upscaling of unsaturated flow in fractured porous media,* J. Math. Anal., 52 (2020), pp. 239–276.

[31] Z. XU, *Homogenization and upscaling for diffusion, heat conduction, and wave propagation in heterogeneous materials,* Commun. Theor. Phys., 57(3) (2012), pp. 348–354.

[32] W. E, B. ENGQUIST, X. LI, W. REN, AND E. VANDEN-EIJNDEN, *Heterogeneous multiscale methods: A review,* Commun. Comput. Phys., 2(3) (2007), pp. 367–450.

[33] E. CHUNG, Y. EFENDIEV, AND W. LEUNG, *Constraint energy minimizing generalized multiscale finite element method,* Comput. Methods Appl. Mech. Eng., 339 (2018), pp. 298–319.

[34] E. CHUNG AND S. PUN, *Online adaptive basis enrichment for mixed CEM-GMSFEM,* Multiscale Model. Simulation, 17 (2019), pp. 1103–1122.

[35] Y. EFENDIEV, J. GALVIS, AND T. HOU, *Generalized multiscale finite element methods (GMS-FEM),* J. Comput. Phys., 251 (2013), pp. 116–135.

[36] Y. EFENDIEV, J. GALVIS, G. LI, AND M. PRESHO, *Generalized multiscale finite element methods: Oversampling strategies,* Int. J. Multiscale Comput. Eng., 12 (2014), pp. 465–484.

[37] T. HOU AND X. WU, *A multiscale finite element method for elliptic problems in composite materials and porous media,* J. Comput. Phys., 134 (1997), pp. 169–189.

[38] T. HOU, X. WU, AND Z. CAI, *Convergence of a multiscale finite element method for elliptic problems with rapidly oscillating coefficients,* Math. Comput., 68 (1999), pp. 913–943.

[39] M. KLIMCZAK AND W. CECOT, *Higher order multiscale finite element method for heat transfer modeling,* Materials (Basel), 14(14) (2021), pp. 27–38.

[40] A. ABDULLE AND G. A. PAVLIOTIS, *Numerical methods for stochastic partial differential equations with multiple scales,* J. Comput. Phys., 231 (2012), pp. 2482–2497.

[41] A. ABDULLE, G. A. PAVLIOTIS, AND U. VAES, *Spectral methods for multiscale stochastic differential equations,* J. Uncertainty Quantification, 5 (2017), pp. 720–761.

[42] P. DOSTERT, Y. EFENDIEV, AND T. HOU, *Multiscale finite element methods for stochastic porous*

media flow equations and application to uncertainty quantification, Comput. Methods Appl. Mech. Eng., 197 (2008), pp. 3445–3455.

[43] B. GANAPATHYSUBRAMANIAN AND N. ZABARAS, *A stochastic multiscale framework for modeling flow through random heterogeneous porous media,* J. Comput. Phys., 228 (2009), pp. 591–618.

[44] X. HE, L. JIANG, AND J. MOULTON, *A stochastic dimension reduction multiscale finite element method for groundwater flow problems in heterogeneous random porous media,* J. Hydrology, 478 (2013), pp. 77–88.

[45] B. LIU, N. VU-BAC, X. ZHUANG, AND T. RABCZUK, *Stochastic multiscale modeling of heat conductivity of polymeric clay nanocomposites,* Mech. Materials, 142 (2020), pp. 103–280.

[46] Z. YANG, X. GUAN, J. CUI, H. DONG, Y. WU, AND J. ZHANG, *Stochastic multiscale heat transfer analysis of heterogeneous materials with multiple random configurations,* Commun. Comput. Phys., 27 (2018), pp. 431–459.

[47] L. BOKAI, V. NAM, AND R. TIMON, *A stochastic multiscale method for the prediction of the thermal conductivity of polymer nanocomposites through hybrid machine learning algorithms,* Compos. Struct., 273 (2021), pp. 114–269.

[48] J. L. LIONS AND E. MAGENES, Non-Homogeneous Boundary Value Problems and Applications. Springer-Verlag, New York, 1972.

[49] X. FENG, Y. LUO, L. VO, AND Z. WANG, *An efficient iterative method for solving parameter-dependent and random diffusion problems,* arXiv preprint arXiv:2105.11901, 1 (2021), pp. 1–25.